

ACCEPTED MANUSCRIPT

Measuring magnetocaloric effect in a phase separated system

To cite this article before publication: Dafne Yael Goijman *et al* 2018 *Mater. Res. Express* in press <https://doi.org/10.1088/2053-1591/aaf04a>

Manuscript version: Accepted Manuscript

Accepted Manuscript is “the version of the article accepted for publication including all changes made as a result of the peer review process, and which may also include the addition to the article by IOP Publishing of a header, an article ID, a cover sheet and/or an ‘Accepted Manuscript’ watermark, but excluding any other editing, typesetting or other changes made by IOP Publishing and/or its licensors”

This Accepted Manuscript is © 2018 IOP Publishing Ltd.

During the embargo period (the 12 month period from the publication of the Version of Record of this article), the Accepted Manuscript is fully protected by copyright and cannot be reused or reposted elsewhere. As the Version of Record of this article is going to be / has been published on a subscription basis, this Accepted Manuscript is available for reuse under a CC BY-NC-ND 3.0 licence after the 12 month embargo period.

After the embargo period, everyone is permitted to use copy and redistribute this article for non-commercial purposes only, provided that they adhere to all the terms of the licence <https://creativecommons.org/licenses/by-nc-nd/3.0>

Although reasonable endeavours have been taken to obtain all necessary permissions from third parties to include their copyrighted content within this article, their full citation and copyright line may not be present in this Accepted Manuscript version. Before using any content from this article, please refer to the Version of Record on IOPscience once published for full citation and copyright details, as permissions will likely be required. All third party content is fully copyright protected, unless specifically stated otherwise in the figure caption in the Version of Record.

View the [article online](#) for updates and enhancements.

Measuring magnetocaloric effect in a phase-separated system.

D. Goijman^{1,4}, A. G. Leyva^{2,3,4}, M. Quintero^{2,3,4}

1- Laboratorio de Resonancias Magnéticas, Gerencia de Física, GAIANN, Centro Atómico Bariloche, Comisión Nacional de Energía Atómica (CNEA), Av Bustillo 9500, Bariloche, Argentina.

2-Departamento de Física de la materia Condensada, GlyAN, GAIANN, Comisión Nacional de Energía Atómica (CNEA), Av. Gral. Paz 1499, San Martin, Buenos Aires, Argentina.

3-Escuela de Ciencia y Tecnología, Universidad Nacional de General San Martin, Alem 3901, San Martin, Buenos Aires, Argentina.

4-Instituto de Nanociencia y Nanotecnología, Av. Gral. Paz 1499, San Martin, Buenos Aires, Argentina.

Abstract.

The magnetocaloric effect (MCE) in a magnetic system can be characterized by the estimation of the entropy change produced when a magnetic field is applied. The discrepancies between the results obtained with different methods have encouraged the scientific community to attempt to better understand the procedures associated with this calculation. Within this context, we present a study about how the presence of an inhomogeneous state influences the determination of the entropy change. To do that we chose a prototypical system used to study the phase separation phenomena in manganites. We compared results obtained using different methods, and we propose an approach to correlate the results obtained following different procedures.

Introduction

The magnetocaloric effect (MCE) is the temperature change produced in a magnetic system when an external magnetic field is applied. Even though the effect was discovered in 1917 by Weiss and Picard[1], the discovery of a large MCE at room temperature in Gd (SiGe) [2] was a new starting point in the study of this effect, which triggered the development of solid state cooling devices based on the MCE. Nowadays, the study of MCE has been extended to a large number of systems, namely Gd nanoparticles [3], As based compounds[4], Heusler alloys[5] [6] and manganites [7] [8]among others.

The MCE can be quantified considering the magnetic entropy change (ΔS) produced by the application of the magnetic field. The entropy change can be obtained from both heat capacity and from magnetization measurements[9], using a Maxwell relation to calculate ΔS by numerical integration of a set of magnetization curves[10].

As the interest in the MCE expanded to a large number of compounds, the methods used to calculate it were carefully revised, especially in those cases where first order phase transitions were involved [11] [12] [13] [14] [15]. The correct application of the Maxwell relation requires a transition between different equilibrium states [16] [17], and its inappropriate use might lead to an overestimation of the entropy change. In order to avoid these undesired effects, some authors propose the use of alternative methods, based on geometric arguments [18] or the Clausius-Clapeyron equation[19]. Another important aspect is the thermodynamic history of the sample. L. Caron et al [16] [20]analyzed the influence of the magnetization measurement protocol in the determination of the entropy change.

Nowadays, despite the advances in the development of direct measurement techniques, the change of entropy is mostly obtained from indirect measurements. Therefore, the study of these techniques is a crucial aspect towards the use of caloric materials for magnetic refrigeration.

1
2
3 From the large number of systems exhibiting MCE, the mixed valence manganese oxides
4 (manganites) are one of the most promising ones, due to their unique ability to tune their
5 magnetic, electric and structural properties by minor modifications in their compositions or in the
6 synthesis parameters (grain size[21], oxygen stoichiometry[22], etc). The strong coupling between
7 the different degrees of freedom in manganites is another aspect to take into account, since it is
8 possible to induce a structural or electrical phase transition by the application of moderate
9 external stimuli (i.e. magnetic field, hydrostatic pressure, radiation).

10
11
12
13
14
15
16
17
18
19
20 The coexistence of regions with different magnetic, electrical and structural properties, the so
21 called phase separation (PS) phenomenon, is one of the most widely studied topics in mixed
22 valence manganese oxides. Despite the enormous efforts made by the scientific community, a
23 complete explanation of the phase coexistence origin is still lacking. The out-of-equilibrium nature
24 of this inhomogeneous state leads to a rich variety of behaviors related to the competition
25 between the different phases. Given this scenario $\text{La}_{0.5}\text{Ca}_{0.5}\text{MnO}_3$ (LCMO) and $\text{La}_{5/8-\gamma}\text{Pr}_\gamma\text{Ca}_{3/8}\text{MnO}_3$
26 (LPCMO) are two prototypical systems where the PS phenomenon has been studied.

27
28
29
30
31
32
33
34
35
36 In LCMO the PS has been studied using different techniques, such as magnetization[23], neutron
37 powder diffraction[24], and many others[25] [26] [27] [28] [29]. In this system, the ferromagnetic
38 metallic (FM) phase competes with the antiferromagnetic (AFM) phase and charge ordering (CO)
39 one, leading to the presence of a dynamic behavior related to the system evolution towards the
40 equilibrium state. By controlling the grain size, it is possible to tune the fraction of the CO phase,
41 through the frustration of the long range order, which favors the stabilization of the FM state [21],
42 while remaining completely suppressed for grain sizes below 15nm[30].

43
44
45
46
47
48
49
50
51
52 In the case of LCMO, the system can be controlled by modifying the Pr/La proportion. In the rich Pr
53 region of the phase diagram, the system is mainly dominated by an AFM and CO phase, while a
54

1
2
3 mainly FM state is observed in the La rich region. For Pr content around 0.3, a strong PS region is
4 present, and has been observed using different techniques [31] [32] [33]. For both systems, the
5 MCE has been studied in order to understand the complex scenario involving the presence of PS in
6 manganites, but also as an example of how the inadequate use of an indirect method can lead to
7 the overestimation of the MCE [34] [35].
8
9
10
11
12
13
14

15 Phan et al [36] analyze the evolution of the entropy change caused by the magnetic field in
16 different temperature ranges in LPCMO, revealing a strong correlation between the entropy
17 change and the system's dynamic behavior. Similarly, Amirzadeh et al [37] studied the MCE in
18 LCMO as a function of grain size, obtaining an anomalous behavior that could be associated with
19 the presence of a magneto-structural transition.
20
21
22
23
24
25
26

27 In this paper, we will discuss the influence of the PS state in the determination of the MCE in
28 manganites. We will compare the results obtained using different methods (Maxwell's relation
29 and heat capacity) and analyze discrepancies and coincidences. Finally we will introduce the
30 necessary modifications to correct the artifacts introduced when the Maxwell relation is applied
31 on an out-of-equilibrium system.
32
33
34
35
36
37
38

39 **Methods**

40
41
42 Polycrystalline $\text{La}_{0.625-y}\text{Pr}_y\text{Ca}_{0.375}\text{MnO}_3$ samples were synthesized using the Sol-gel technique and
43 characterized by X-Ray diffraction to confirm composition, structure and to ensure good quality.
44 Magnetic measurements were performed using the vibrating sample magnetometry technique,
45 and heat capacity was measured using adiabatic relaxation in a Versalab system manufactured by
46 Quantum Design. In all the results presented in this paper, magnetization as a function of
47 temperature was measured on cooling with the applied magnetic field and a cooling rate of 1
48 K/min. in sweep mode. Isothermal magnetization loops were measured after cooling the sample
49
50
51
52
53
54
55
56
57
58
59
60

1
2
3 without an applied magnetic field, starting at room temperature (the sample was always warmed
4 up to room temperature between measurements).
5
6

7
8 Heat capacity measurements were taken on cooling, with a variable cooling rate due to the
9 characteristics of the adiabatic relaxation method, which requires temperature stability.
10
11

12 13 14 **Results**

15
16 The phase diagram for $\text{La}_{0.625-\gamma}\text{Pr}_{\gamma}\text{Ca}_{0.375}\text{MnO}_3$, schematized in Figure 1, can be divided in three
17 regions, varying in Pr content (γ). In the low γ region ($\gamma < 0.20$), the system presents a
18 ferromagnetic metallic (FMM) behavior for temperatures below $T_c \sim 230$ K. The magnetization
19 value obtained for the sample with $\gamma=0.20$ (LPC-20) (fig 2a) is consistent with the complete
20 alignment of the Mn ions. In the magnetization as a function of magnetic field curves it is possible
21 to see how the paramagnetic state give place to the FM state as the temperature decreases.
22
23
24
25
26
27
28
29

30
31 On the opposite side, for $\gamma > 0.5$ a charge order (CO) appears at $T_{co} \sim 210$ K on cooling. Some
32 degrees below, the Mn ions are anti-ferromagnetically ordered (AFM)[38]. The magnetization
33 values obtained for the sample with $\gamma = 0.50$ (LPC-50) (fig2 c) are one order of magnitude smaller
34 than the ones observed for the ferromagnetic ordering. The corresponding magnetization as a
35 function of the magnetic field measurements confirms the presences of the mentioned phases.
36
37
38
39
40
41
42

43 In the intermediate region, the system is characterized by the presence of the phase separation
44 (PS) state. In figure 2b, we present magnetization as a function of temperature for the sample
45 with $\gamma = 0.32$ (LPC-32)). The room temperature state of the system is paramagnetic insulator, as
46 can be seen in the linear behavior of the magnetization as a function of magnetic field curves. On
47 cooling, the CO phase appears at $T_{co} = 220$ K and some degrees below, at $T_c \sim 200$ K, the
48 magnetization increases, indicating the formation of FM regions. The presence of an
49
50
51
52
53
54
55
56
57
58
59
60

1
2
3 inhomogeneous state can be observed in the magnetization as a function of magnetic field
4
5 curves, characterized by a two step increase. The system maintains an almost constant
6
7 magnetization value, and down to $T \sim 100$ K, where the magnetization values present an abrupt
8
9 increase, reaching values consistent with a homogeneous FM state at lower temperatures. In
10
11 order to understand how the behavior described above is reflected in magnetocaloric properties,
12
13 it is necessary to determine the entropy change. Following the most commonly accepted
14
15 approach, it is possible to estimate this change using numerical integration of magnetization loops
16
17 at different temperatures as
18
19

$$\Delta S_M = \frac{1}{\Delta T} \int_0^H [M(T + \Delta T, H') - M(T, H')] dH' \quad (1)$$

20
21
22
23
24
25
26
27 being M and H the magnetization and the applied magnetic field, respectively.
28
29

30 In Figure 3 we show the temperature dependence of the entropy change obtained from the M (H)
31
32 branch measured increasing H from 0 to 3 T. In order to avoid the “peak effect” usually observed
33
34 around first order transitions, we warmed up the samples above Curie temperature after each
35
36 magnetization loop measurement [16].
37
38

39
40 For LPC-20 and LPC-32 samples, H is strong enough to suppress the CO phase and leads to a
41
42 homogeneous FM, in contrast to what happens with LPC-50, where the magnetic field does not
43
44 convert the CO/AFM phase to FM.
45
46

47 For LPC-20, the entropy displays a peak at 235 K with a value of 9 J/Kg. K, which is consistent with
48
49 the PI to FM transition, and close to the values already reported [8]. The LPC-50 sample presents
50
51 two peaks, one of 0.3 J/Kg K at 235 K, and another one which is three times smaller, at 170 K. The
52
53
54
55
56
57
58
59
60

1
2
3 first one is associated with the formation of the CO phase, and the second one is related to the
4 AFM ordering[39].
5

6
7
8 In the case of LPC-32, two peaks are observed at 110 K and 210 K with a value of 6 J/kg. K, in line
9 with the behavior observed in a system with a similar composition[36] . Both peaks are correlated
10 with the transitions observed in M (T) at those temperatures.
11
12
13

14
15
16 The heat capacity measured at constant magnetic field and pressure (C_p) values enabled us to
17 determine total entropy, and it is possible to determine the entropy change from two C_p curves as
18
19

$$20 \Delta S_{HC}(T, H) = \int_{T_0}^T \frac{C_p(T', H) - C_p(T', H = 0)}{T'} dT' + \Delta S(T_0, H) \quad (2)$$

21
22 where
23

24
25
26 $C_p(T, H)$ is the heat capacity at constant pressure
27

28
29
30 $\Delta S(T_0, H)$ is the difference in zero temperature entropies.
31

32
33
34 In Figure 4 we show the entropy change (ΔS_{HC}) as a function of temperature for samples LPC-20,
35 LPC-32 and LPC-50 obtained from heat capacity curves. In all the cases, the lowest temperature
36 reached was 50K.
37
38
39

40
41
42 For LPC-20 and LPC-50, $\Delta S_{HC}(50K)$ was considered as zero for different reasons. In the first
43 case, the sample is a soft FM and at 50 K the magnetic moments are completely aligned at zero
44 field. In the second case, the maximum applied H is not enough to modify the CO phase.
45
46
47
48

49
50
51 In the case of LPC-32, the value of $\Delta S_{HC}(50K)$ was obtained comparing the entropy change in
52 the high temperature paramagnetic phase with the value obtained from $\Delta S_M(T)$. The result
53
54
55
56
57
58
59
60

1
2
3 $\Delta S_{HC}(50K) = -6.74 J / KgK$ is consistent with the values measured during a FM to CO
4 transition in similar samples[40] [41].
5
6

7 8 **Discussion**

9
10 We observe a good agreement between the results obtained using Maxwell's relation and the
11 heat capacity for samples LPC-20 and LPC-50.
12
13

14 Comparing $\Delta S_{HC}(T)$ and $\Delta S_M(T)$ for LPC-32, we observed substantial differences below 210 K.
15
16

17 These discrepancies could be related to the use of Maxwell's relation under inadequate
18 conditions, such as the coexistence of two different phases and possible hysteresis losses .
19
20

21 In order to analyze the contribution of each of the abovementioned effects, we proposed the
22 following modifications to the expression for ΔS obtained using Maxwell's relations.
23
24

25 The first modification takes into account the inhomogeneous state observed in the intermediate
26 region. When the entropy change is calculated for a certain temperature using the numerical
27 integration for equation 1, the result obtained is mainly due to the magnetization change at the PI-
28 FM transition, but it is also affected by the change in the relative fraction of the FM phase (f) [13].
29
30

31 The temperature dependence of f can be extracted from the magnetization as a function of
32 temperature, and it can be initially normalized with the magnetization of the entire Mn network
33 aligned with the magnetic field.
34
35

36 Then
37
38

$$39 \Delta S_{MOD}(T) = \Delta S_H(T) + \alpha \cdot f(T) \quad (3)$$

40 where
41
42
43
44
45
46
47
48
49
50

$\Delta S_{MOD}(T)$ is the modified entropy change

$\Delta S_H(T)$ is the entropy corresponding to the homogeneous system.

The other contribution to be considered is energy losses due to the presence of hysteresis in the $M(H)$ curves, which can be related to the presence of defects such as grain boundary, tangles of dislocation, precipitates or inhomogeneities that hinder the advance of the domain walls, preventing the system from reaching the global energy state [42].

To analyze the effect of the hysteresis, we will assume that the system's equilibrium state will be a reversible curve named M_{AN} in Figure 5. The hysteretic magnetization curve can be separated in two different branches, one obtained when the magnetic field is increased (M_{\uparrow}) and the other one corresponding to a decrease in the magnetic field (M_{\downarrow}). For simplicity's sake, we chose for M_{AN} to be in the center of the hysteresis loop, so we that we could introduce a parameter (δ) to quantify the hysteresis as:

$$M_{\uparrow} = M_{AN} - \delta \quad (4a)$$

$$M_{\downarrow} = M_{AN} + \delta \quad (4b)$$

When the entropy change is calculated using Maxwell's relation, it is usually calculated based on M_{\uparrow} curves. Then, it can be expressed as a function of M_{AN} as:

$$\Delta S_M = \frac{1}{\Delta T} \int_0^H [M_{AN}(H', T + \Delta T) - \delta(H', T + \Delta T) - M_{AN}(H', T) + \delta(H', T)] dH' \quad (5)$$

Introducing the magnetic work (W) as the area enclosed by M_{\uparrow} and M_{\downarrow} , it can be expressed in terms of δ :

$$W(T) = 2 \int_0^H \delta(H', T) dH' \quad (6)$$

The inset in Figure 5 shows W as a function of temperature for a maximum magnetic field of 3 T for LPC-32. The magnetic work presents a very low value (almost zero) at temperatures above 225 K, in the paramagnetic region at low magnetic signals. In the opposite sense, the low W values observed at low temperatures are consistent with the almost homogeneous low temperature ferromagnetic state. We observed high values in the intermediate temperature region, where the PS state is fully established; these high values could be associated with the nucleation of the CO phase, which competes with the FM phase, acting as pinning centers for the displacement of domain walls and the borders of the FM regions. Once the FM energy is enough to overcome the CO phase, the whole sample converts abruptly to the FM phase and no more extra W is needed.

The expression for the entropy change can be expressed as:

$$\Delta S_M = \Delta S_{AN} - \frac{1}{2} \frac{\partial W}{\partial T} \quad (7)$$

The expressions presented in equations 3 and 7 consider the entropy change calculated using Maxwell's relation for the case of an inhomogeneous and hysteretic system. Note that in the case of a homogeneous system, the FM fraction is constant below the critical temperature and no hysteresis appears in the magnetization curves, making equations 3 and 7 turn into ΔS_H .

Taking into account the scenario described above, we will attempt to use it to explain the large difference between ΔS obtained from MR and from heat capacity measurements. In that sense we collapsed the abovementioned contributions in the following expression:

$$\Delta S_M^*(T_i) = \Delta S_{HC}(T) + \alpha f(T) - \beta \frac{\partial W}{\partial T}(T) \quad (8)$$

In order to find the maximum likelihood between ΔS_M^* and ΔS_M , we studied the statistical distance between both expressions. The residual r at a given temperature T_i can be defined as

$$r_{\alpha\beta}(T_i) = \Delta S_{HC}(T_i) + \alpha f(T_i) - \beta \frac{\partial W}{\partial T}(T_i) - \Delta S_M(T_i) \quad (9)$$

The estimation of α and β can be obtained by minimizing the function

$$\xi(\alpha, \beta) = \sum_i r_{\alpha\beta}^2(T_i) \quad (10)$$

being i the index for the measured point (in our case, between 50 K and 300K).

Numerically evaluating ξ for α between -1 and 4 (with a step of 0.01) and β between -20 to 50 (with a step of 0.1), we reached the minimum values for

$$\alpha = (10.8 \pm 0.1) \frac{J}{KgK} \text{ and}$$

$$\beta = (0.46 \pm 0.01).$$

It is interesting to note that the value obtained for α is close to the maximum entropy change obtained for the sample with $\gamma = 0.2$ (9 J/KgK), corresponding to the full FM sample. Additionally, the value obtained for parameter β is close to the value predicted in equation 5 (0.5).

In figure 6 we compare the temperature dependence of the entropy change measured using MR and HC and the one calculated from the optimized parameters in equation 8. It can be observed that there is a very good agreement between the results obtained from MR and those extracted by using equation 8.

Conclusions

Summarizing, in this paper we studied the influence of the phase separation phenomenon in magnetocaloric properties in samples of the $\text{La}_{0.625-\gamma}\text{Pr}_{\gamma}\text{Ca}_{0.375}\text{MnO}_3$ family. To do that we used three different samples (a FM homogeneous (LPC-20), a CO/AFM (LPC-50) and a phase separated (LPC-32)). Comparing the results obtained using two alternative experimental methods to

1
2
3 calculate the entropy change, we observed a good agreement between both methods for the
4 homogeneous samples. However, a great difference between both methods was observed for the
5 phase separated sample. In order to understand the origin of this discrepancy, we improved the
6 model by including two additional terms to the entropy change, which consider the effect of an
7 inhomogeneous state and the hysteresis loops present at the M (H) curves. Considering these two
8 contributions, it was possible to reach the entropy change using MR, and taking the heat capacity
9 entropy change as the starting point.
10
11
12
13
14
15
16
17
18

19 **Acknowledgments**

20 This paper has been possible thanks to the support from ANPCyT PICT 1506/2012 and 2016/2014.

21 We wish to thank L. Granja for reading the manuscript and I. Urrutia and L. Fernandez Piana for
22 their contributions in fruitful discussions. M.O. is also a member of CIC-CONICET.
23
24
25
26
27
28
29
30
31
32
33
34
35
36
37
38
39
40
41
42
43
44
45
46
47
48
49
50
51
52
53
54
55
56
57
58
59
60

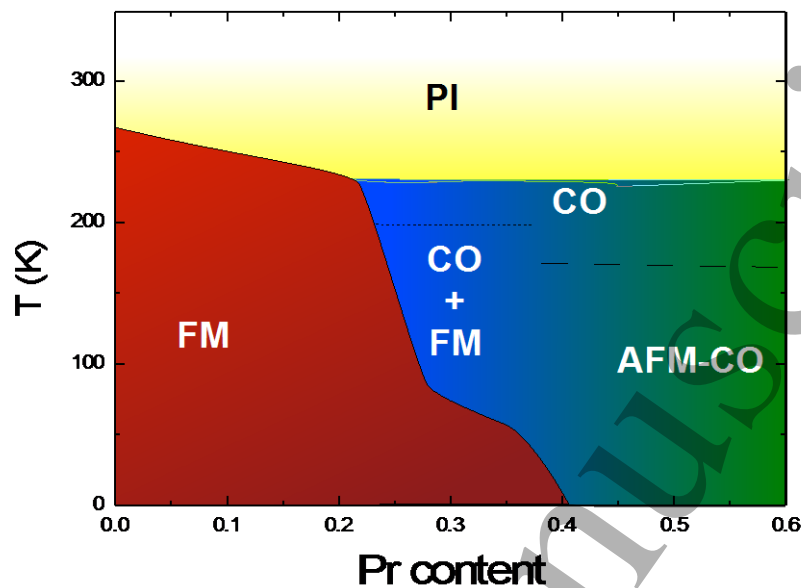


Figure 1: Magnetic phase diagram of $\text{La}_{0.625-y}\text{Pr}_y\text{Ca}_{0.375}\text{MnO}_3$ (FM: ferromagnetic metallic, CO: charge ordered, PI: paramagnetic insulator and AFM: antiferromagnetic).

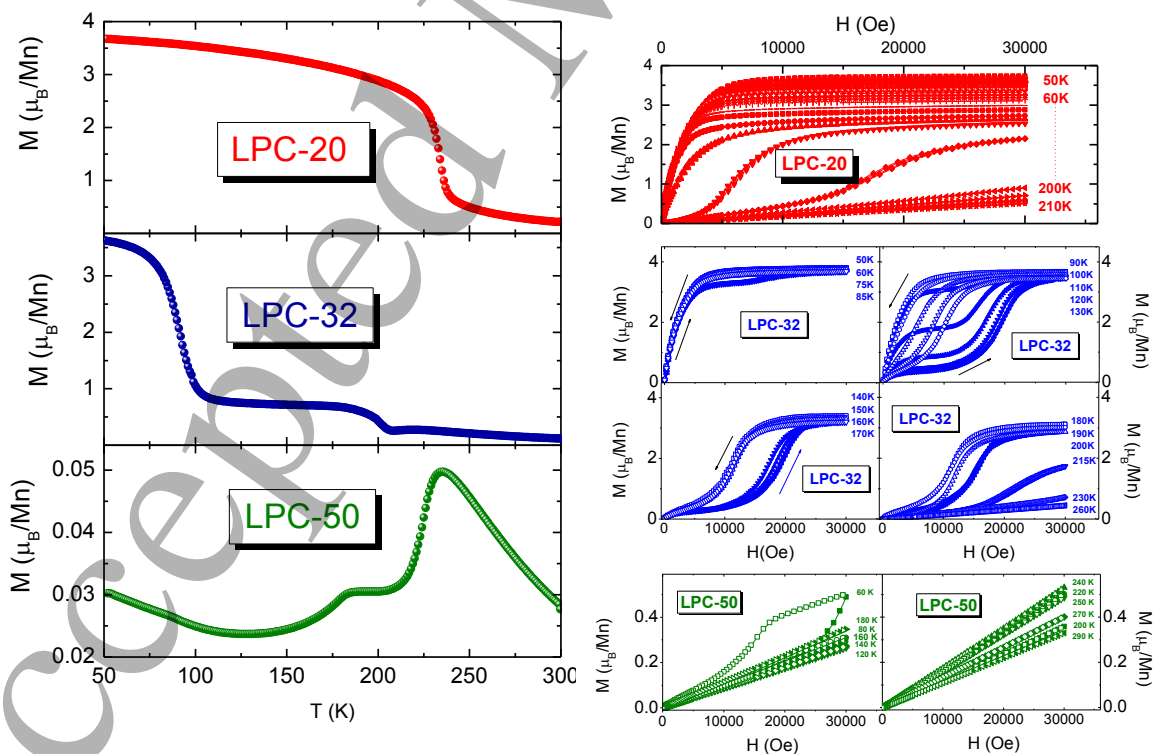


Figure 2: Magnetization as a function of temperature (left) and as a function of magnetic field (right) for samples $\text{La}_{0.625-\gamma}\text{Pr}_{\gamma}\text{Ca}_{0.375}\text{MnO}_3$ with $\gamma = 0.2$ (upper panel), $\gamma = 0.32$ (middle panel) and $\gamma = 0.5$ (lower panel). Solid (open) symbols indicate that the magnetic field is increasing (decreasing). Magnetization as a function of the magnetic field curves (right) for samples with $\gamma=0.2$ (upper), $\gamma=0.32$ (middle) and $\gamma=0.5$ (lower). The temperature of the curves are indicated.

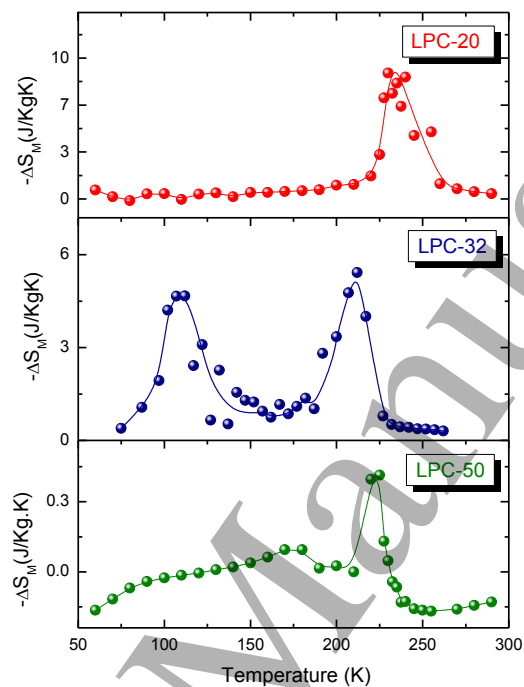


Figure3: Entropy change (from Maxwell's relation) as a function of temperature for samples $\text{La}_{0.625-\gamma}\text{Pr}_{\gamma}\text{Ca}_{0.375}\text{MnO}_3$ with $\gamma = 0.2$ (upper panel), $\gamma = 0.32$ (middle panel) and $\gamma = 0.5$ (lower panel).

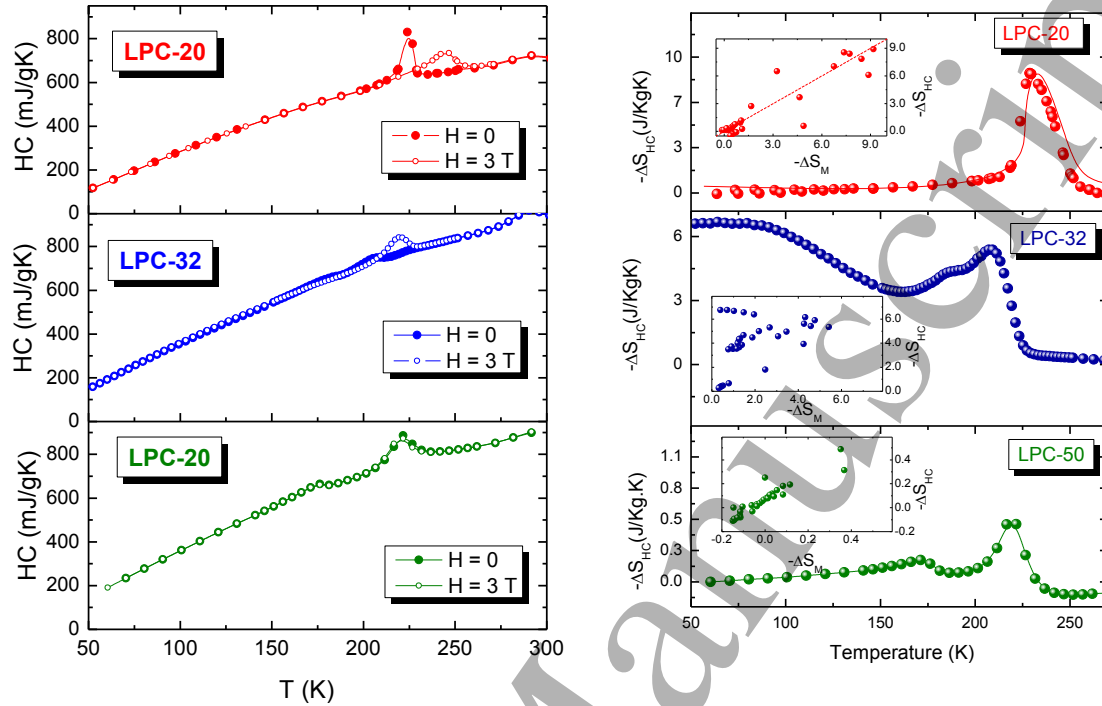


Figure 4: (Left) Heat capacity as a function of temperature and (right) entropy change (from heat capacity measurements) as a function of temperature for samples $\text{La}_{0.625-\gamma}\text{Pr}_{\gamma}\text{Ca}_{0.375}\text{MnO}_3$ with $\gamma = 0.2$ (upper panel), $\gamma = 0.32$ (middle panel) and $\gamma = 0.5$ (lower panel). In the insets, ΔS_M and ΔS_{HC} are compared.

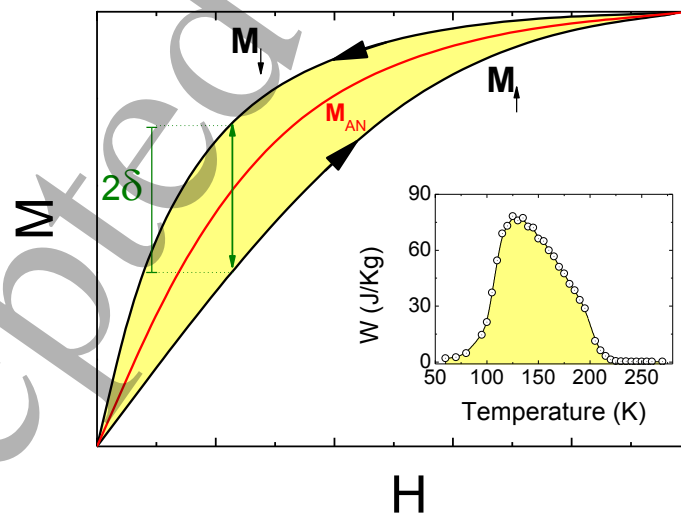


Figure 5: Schematic representation of an isothermal magnetization loop, where M_{\uparrow} and M_{\downarrow} are the two branches corresponding to increases and decreases in the magnetic field. M_{AN} . The inset shows the temperature dependence of the magnetic work (W) defined as the area enclosed between M_{\uparrow} and M_{\downarrow} for the sample with $\gamma = 0.32$

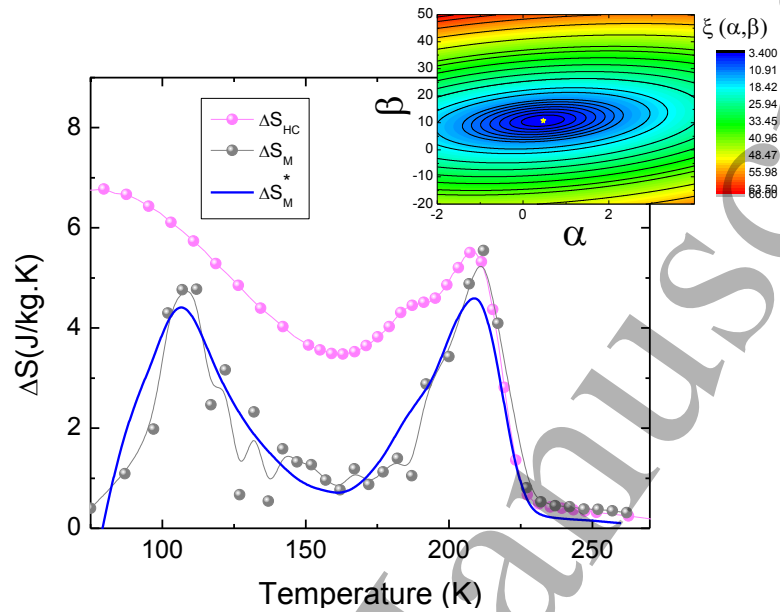


Figure 6: Entropy change as a function of temperature extracted from magnetization curves (gray), from heat capacity (pink) and from equation 8 (blue) for sample with $\gamma = 0.32$. The inset shows a color map of the error function ξ used to obtain optimized α and β values.

- [1] Weiss, Pierre and Piccard, Auguste, "Le phénomène magnétocalorique," *J. Phys. Theor. Appl.*, vol. 7, no. 1, pp. 103–109, 1917.
- [2] V. K. Pecharsky and K. A. Gschneidner Jr., "Giant Magnetocaloric Effect in $Gd_5Si_2Ge_2$," *Phys. Rev. Lett.*, vol. 78, no. 23, pp. 4494–4497, Jun. 1997.
- [3] H. Zeng, J. Zhang, C. Kuang, and M. Yue, "Magnetic entropy change in bulk nanocrystalline Gd metals," *Appl. Nanosci.*, vol. 1, no. 1, pp. 51–57, May 2011.
- [4] H. Wada and Y. Tanabe, "Giant magnetocaloric effect of $MnAs_{1-x}Sb_x$," *Appl. Phys. Lett.*, vol. 79, no. 20, pp. 3302–3304, 2001.
- [5] A. Planes, L. Mañosa, X. Moya, T. Krenke, M. Acet, and E. F. Wassermann, "Magnetocaloric effect in Heusler shape-memory alloys," *J. Magn. Magn. Mater.*, vol. 310, no. 2, Part 3, pp. 2767–2769, 2007.
- [6] C. S. Mejía, A. M. Gomes, and L. A. S. de Oliveira, "A less expensive NiMnGa based Heusler alloy for magnetic refrigeration," *J. Appl. Phys.*, vol. 111, no. 7, p. 07A923, 2012.
- [7] M. H. Phan and S. C. Yu, "Review of the magnetocaloric effect in manganite materials," *J. Magn. Magn. Mater.*, vol. 308, no. 2, pp. 325–340, 2007.
- [8] A. Rebello, V. B. Naik, and R. Mahendiran, "Large reversible magnetocaloric effect in $La_{0.7-x}Pr_xCa_{0.3}MnO_3$," *J. Appl. Phys.*, vol. 110, no. 1, pp. 1–7, 2011.
- [9] J. Pecharsky VK, Gschneidner KA, "Magnetocaloric effect from indirect measurements: magnetization and heat capacity.," *J. Appl. Phys.*, vol. 86, no. 1999, pp. 565–75, 1999.
- [10] M. Földeàki, R. Chahine, T. K. Bose, and M. Fiildeiki, "Magnetic measurements : A powerful tool in magnetic refrigerator design measurements : A powerful tool in magnetic refrigerator design," vol. 3528, no. May 2013, 1995.
- [11] N. A. de Oliveira and P. J. von Ranke, "Magnetocaloric effect around a magnetic phase transition," *Phys. Rev. B*, vol. 77, no. 21, p. 214439, Jun. 2008.
- [12] A. M. G. Carvalho, A. A. Coelho, P. J. von Ranke, and C. S. Alves, "The isothermal variation of the entropy (ΔS) may be miscalculated from magnetization isotherms in some cases: MnAs and $Gd_5Ge_2Si_2$ compounds as examples," *J. Alloys Compd.*, vol. 509, no. 8, pp. 3452–3456, 2011.
- [13] W. Cui, W. Liu, and Z. Zhang, "The origin of large overestimation of the magnetic entropy changes calculated directly by Maxwell relation," *Appl. Phys. Lett.*, vol. 96, no. 22, pp. 1–4, 2010.
- [14] G. Porcari *et al.*, "Convergence of direct and indirect methods in the magnetocaloric study of first order transformations: The case of Ni-Co-Mn-Ga Heusler alloys," *Phys. Rev. B - Condens. Matter Mater. Phys.*, vol. 86, no. 10, pp. 1–5, 2012.

- 1
2
3 [15] J. S. Amaral and V. S. Amaral, "On estimating the magnetocaloric effect from magnetization
4 measurements," *J. Magn. Magn. Mater.*, vol. 322, no. 9–12, pp. 1552–1557, 2010.
5
6 [16] L. Caron, Z. Q. Ou, T. T. Nguyen, D. T. Cam Thanh, O. Tegus, and E. Brück, "On the
7 determination of the magnetic entropy change in materials with first-order transitions," *J.*
8 *Magn. Magn. Mater.*, vol. 321, no. 21, pp. 3559–3566, 2009.
9
10 [17] J. R. Sun, F. X. Hu, and B. G. Shen, "Comment on "Direct Measurement of the "Giant"
11 Adiabatic Temperature Change in $Gd_5Si_2Ge_2$," *Phys. Rev. Lett.*, vol. 85, no. 19, p. 4191,
12 Nov. 2000.
13
14 [18] G. J. Liu *et al.*, "Determination of the entropy changes in the compounds with a first-order
15 magnetic transition," *Appl. Phys. Lett.*, vol. 90, no. 3, p. 32507, 2007.
16
17 [19] A. Giguère *et al.*, "Direct Measurement of the 'Giant' Adiabatic Temperature Change in Gd
18 $5Si_2Ge_2$," pp. 11–14, 1999.
19
20 [20] L. Caron, N. Ba Doan, and L. Ranno, "On entropy change measurements around first order
21 phase transitions in caloric materials," *J. Phys. Condens. Matter*, vol. 29, no. 7, 2017.
22
23 [21] P. Levy *et al.*, "Controlled phase separation in $La_{0.5}Ca_{0.5}MnO_3$," *Phys. Rev. B*, vol. 62, no.
24 10, pp. 6437–6441, Sep. 2000.
25
26 [22] A. Shahee and N. P. Lalla, "Oxygen stoichiometry: A key parameter to tune structural phase
27 diagram of $La_{0.2}Sr_{0.8}MnO_{3-\delta}$," *AIP Conf. Proc.*, vol. 1665, no. 1, p. 30005, 2015.
28
29 [23] R. S. Freitas, L. Ghivelder, P. Levy, and F. Parisi, "Magnetization studies of phase separation
30 in $La_{0.5}Ca_{0.5}MnO_3$," *Phys. Rev. B*, vol. 65, no. 10, p. 104403, Feb. 2002.
31
32 [24] Q. Huang *et al.*, "Temperature and field dependence of the phase separation, structure,
33 and magnetic ordering in $La_{1-x}Ca_xMnO_3$ ($x=0.47, 0.50, \text{ and } 0.53$)," *Phys. Rev. B*, vol. 61, no.
34 13, pp. 8895–8905, 2000.
35
36 [25] J. Mira, J. Rivas, L. E. Hueso, F. Rivadulla, and M. A. López Quintela, "Drop of
37 magnetocaloric effect related to the change from first- to second-order magnetic phase
38 transition in $La_{2/3}(Ca_{1-x}Sr_x)_{1/3}MnO_3$," *J. Appl. Phys.*, vol. 91, no. 10 I, pp. 8903–8905,
39 2002.
40
41 [26] F. Rivadulla *et al.*, "Coexistence of paramagnetic-charge-ordered and ferromagnetic-
42 metallic phases in $La_{0.5}Ca_{0.5}MnO_3$ evidenced by electron spin resonance," *J. Appl. Phys.*,
43 vol. 91, no. 2, pp. 785–788, 2002.
44
45 [27] M. Kim *et al.*, "Raman scattering studies of temperature- and field-induced melting of
46 charge order in $(La,Pr,Ca)MnO_3$," pp. 1–13, 2008.
47
48 [28] C. H. Chen and S.-W. Cheong, "Commensurate to Incommensurate Charge Ordering and Its
49 Real-Space Images in $La_{0.5}Ca_{0.5}MnO_3$," *Phys. Rev. Lett.*, vol. 76, no. 21, pp. 4042–4045,
50 May 1996.
51
52 [29] S. Mori, C. H. Chen, and S.-W. Cheong, "Paired and Unpaired Charge Stripes in the
53 Ferromagnetic Phase of $La_{0.5}Ca_{0.5}MnO_3$," *Phys. Rev. Lett.*, vol. 81, no. 18, pp. 3972–
54 3975, Nov. 1998.
55
56
57
58
59
60

- 1
2
3 [30] T. Sarkar, B. Ghosh, A. K. Raychaudhuri, and T. Chatterji, "Crystal structure and physical
4 properties of half-doped manganite nanocrystals of less than 100-nm size," *Phys. Rev. B -*
5 *Condens. Matter Mater. Phys.*, vol. 77, no. 23, 2008.
- 6
7 [31] M. Uehara, S. Mori, C. H. Chen, and S.-W. Cheong, "Percolative phase separation underlies
8 colossal magnetoresistance in mixed-valent manganites," *Nature*, vol. 399, p. 560, Jun.
9 1999.
- 10
11 [32] W. Wu, C. Israel, N. Hur, S. Park, S.-W. Cheong, and A. de Lozanne, "Magnetic imaging of a
12 supercooling glass transition in a weakly disordered ferromagnet," *Nat. Mater.*, vol. 5, p.
13 881, Oct. 2006.
- 14
15 [33] W. Kundhikanjana *et al.*, "Direct Imaging of Dynamic Glassy Behavior in a Strained
16 Manganite Film," *Phys. Rev. Lett.*, vol. 115, no. 26, pp. 1–5, 2015.
- 17
18 [34] M. Quintero, S. Passanante, I. Irurzun, D. Goijman, and G. Polla, "Grain size modification in
19 the magnetocaloric and non-magnetocaloric transitions in La_{0.5}Ca_{0.5}MnO₃ probed by
20 direct and indirect methods," *Appl. Phys. Lett.*, vol. 105, no. 15, 2014.
- 21
22 [35] M. Quintero, J. Sacanell, L. Ghivelder, A. M. Gomes, A. G. Leyva, and F. Parisi,
23 "Magnetocaloric effect in manganites: Metamagnetic transitions for magnetic
24 refrigeration," *Appl. Phys. Lett.*, vol. 97, no. 12, 2010.
- 25
26 [36] M. H. Phan, M. B. Morales, N. S. Bingham, H. Srikanth, C. L. Zhang, and S. W. Cheong,
27 "Phase coexistence and magnetocaloric effect in La_{5/8-y}PryCa_{3/8}MnO₃," *Phys. Rev. B*,
28 vol. 81, no. 9, p. 94413, 2010.
- 29
30 [37] P. Amirzadeh *et al.*, "Phase separation and direct magnetocaloric effect in La_{0.5}Ca_{0.5}MnO₃
31 manganite," *J. Appl. Phys.*, vol. 113, no. 12, p. 123904, 2013.
- 32
33 [38] J. M. D. Coey, M. Viret, and S. von Molnár, "Mixed-valence manganites – ten years on,"
34 *Adv. Phys.*, vol. 58, no. 6, pp. 567–569, Nov. 2009.
- 35
36 [39] Z. Jiráček, S. Krupička, Z. Šimša, M. Dlouhá, and S. Vratislav, "Neutron diffraction study of Pr₁
37 – xCa_xMnO₃ perovskites," *J. Magn. Magn. Mater.*, vol. 53, no. 1, pp. 153–166, 1985.
- 38
39 [40] L. Ghivelder *et al.*, "Abrupt field-induced transition triggered by magnetocaloric effect in
40 phase-separated manganites," *Phys. Rev. B - Condens. Matter Mater. Phys.*, vol. 69, no. 21,
41 2004.
- 42
43 [41] A. L. L. Sharma, P. A. Sharma, S. K. McCall, S. B. Kim, and S. W. Cheong, "Enhanced magnetic
44 refrigeration capacity in phase separated manganites," *Appl. Phys. Lett.*, vol. 95, no. 9, pp.
45 95–97, 2009.
- 46
47 [42] D. C. Jiles and D. L. Atherton, "Theory of the magnetisation process in ferromagnets and its
48 application to the magnetomechanical effect," *J. Phys. D. Appl. Phys.*, vol. 17, no. 6, pp.
49 1265–1281, 1984.
- 50
51
52
53
54
55
56
57
58
59
60